

# Utilization of Heme as an Iron Source by Marine *Alphaproteobacteria* in the *Roseobacter* Clade

Kelly L. Roe,\* Shane L. Hogle, Katherine A. Barbeau

Geoscience Research Division, Scripps Institution of Oceanography, La Jolla, California, USA

The bioavailability and utilization of porphyrin-bound iron, specifically heme, by marine microorganisms have rarely been examined. This study used *Ruegeria* sp. strain TrichCH4B as a model organism to study heme acquisition by a member of the *Roseobacter* clade. Analogs of known heme transporter proteins were found within the *Ruegeria* sp. TrichCH4B genome. The identified heme uptake and utilization system appears to be functional, as the heme genes were upregulated under iron stress, the bacterium could grow on ferric-porphyrin complexes as the sole iron source, and internalization of  $^{55}\text{Fe}$  from ferric protoporphyrin IX was observed. The potential ability to utilize heme in the *Roseobacter* clade appears to be common, as half of the isolates in the RoseoBase database were found to have a complete heme uptake system. A degenerate primer set was designed and successfully used to identify the putative heme oxygenase gene (*hmus*) in the *Roseobacter* heme uptake system from diverse nonenriched marine environments. This study found that members of the *Roseobacter* clade are capable of utilizing heme as an iron source and that this capability may be present in all types of marine environments. The results of this study add a new perspective to the current picture of iron cycling in marine systems, whereby relatively refractory intracellular pools of heme-bound iron may be taken up quickly and directly reincorporated into living bacteria without previous degradation or the necessity of a siderophore intermediate.

For microbes in the surface ocean, iron is considered a limiting nutrient in many regions where macronutrients are in excess. The dissolved iron in the surface ocean that is available to marine microorganisms is almost exclusively (>99%) bound to organic ligands (1–4). Iron-ligand complexes are likely important sources of iron for marine bacteria, as model organisms have been observed to acquire iron from iron-ligand complexes (5–9), including siderophores [iron(III) binding ligands secreted by bacteria]. However, the bioavailability of other iron-ligand complexes, such as heme or ferric protoporphyrin IX, to marine microbes has largely been overlooked.

Heme is a common intracellular iron binding molecule that is biologically important as the prosthetic group in many hemoproteins, such as hemoglobin and cytochromes (10). In cultured marine phytoplankton and heterotrophic bacteria, heme can account for up to 40% of the cellular iron concentration (11, 12). The release of these intracellular pools of heme-containing molecules (including hemoproteins) into the water column by cell destruction processes (i.e., zooplankton grazing, viral lysis, or bacterial degradation of detritus) may represent a pathway for efficient iron recycling in the upper ocean, where iron concentrations can be low (subnanomolar levels).

Once released into the extracellular environment, heme complexes are likely to be found on surfaces or in particles due to the hydrophobicity of the heme moiety at oceanic pH values. In the marine environment, heme has been detected at picomolar concentrations in particulate material (13) and at nanomolar concentrations in the dissolved phase in estuaries (14). Heme is also susceptible to photochemical degradation in the surface ocean; thus, heme accumulation is presumably limited to low-light environments.

The bioavailability of heme as an iron source has been well studied for pathogens (8), but thus far it has only been examined in a few marine bacterial isolates (6, 15, 16). The acquisition of exogenous heme by pathogenic bacteria is similar to the high-affinity transport system of siderophores (8). The heme acquisition

system is comprised of a TonB complex (ExbB, ExbD, and TonB), an outer membrane receptor (HmuR), and an ABC (ATP binding cassette) transport system, which consists of a periplasmic binding protein (HmuT), a membrane permease (HmuU), and an ATPase (HmuV). One important feature specific to the heme acquisition system is the heme oxygenase and/or chaperone protein (HmuS), located in the cytoplasm, which appears to be necessary to successfully utilize the iron from heme complexes in characterized systems. Similar systems have been identified in two marine isolates, *Microscilla marina* (*Flexibacteriaceae*) (15) and *Vibrio fischeri* (16), and identifiable heme outer membrane receptors have been located in genomes from diverse taxonomic groups of non-pathogenic marine bacteria (15), suggesting that heme utilization may not be pathogen specific.

The aim of this study was to increase our understanding of heme uptake as a microbial iron acquisition strategy in the marine environment, focusing on the bioavailability of heme complexes to bacteria in the diverse *Roseobacter* clade (17, 18). The presence of putative heme receptors and heme oxygenase genes within this clade suggests that heme utilization is a possibility (15). The isolate *Ruegeria* sp. strain TrichCH4B was used in this study as a model representative strain to examine whether heme complexes are a bioavailable iron source to marine *Roseobacter*. Further insight into heme utilization in the *Roseobacter* clade was obtained

Received 13 May 2013 Accepted 3 July 2013

Published ahead of print 19 July 2013

Address correspondence to Katherine A. Barbeau, kbarbeau@ucsd.edu.

\* Present address: Kelly L. Roe, Department of Chemistry and Geochemistry, Colorado School of Mines, Golden, Colorado, USA.

Supplemental material for this article may be found at <http://dx.doi.org/10.1128/AEM.01562-13>.

Copyright © 2013, American Society for Microbiology. All Rights Reserved.

doi:10.1128/AEM.01562-13

by searching the genomes of roseobacter isolates for the presence of a complete heme uptake system and detection of the heme uptake gene *hmuS* by degenerate primers in the natural roseobacter population in diverse marine habitats.

## MATERIALS AND METHODS

**Culture and growth conditions.** *Ruegeria* sp. TrichCH4B were maintained in 1/10 SWC medium (750 ml of 0.2- $\mu$ m-filtered seawater, 250 ml Milli-Q, 0.5 g Bacto peptone, 0.3 g yeast extract, 6 ml 50% glycerol, 50 mM Tris; pH 7.5). The genome of TrichCH4B is publicly available in the NCBI database (reference ID ACNZ000000000). The experimental cultures were grown under iron-limiting conditions in PC medium as described in detail in reference 9. Briefly, PC medium was composed of 1 liter of 0.2- $\mu$ m-filtered seawater, 1 g Bacto peptone, 1 g casein,  $4.7 \times 10^{-3}$  M  $\text{NH}_4\text{Cl}$ ,  $6.6 \times 10^{-4}$  M  $\text{KH}_2\text{PO}_4$ ,  $5.0 \times 10^{-5}$  M  $\text{Na}_2\text{EDTA}$ ,  $4.0 \times 10^{-8}$  M  $\text{ZnSO}_4$ ,  $2.3 \times 10^{-7}$  M  $\text{MnCl}_2$ ,  $2.5 \times 10^{-8}$  M  $\text{CoCl}_2$ ,  $1.0 \times 10^{-8}$  M  $\text{CuSO}_4$ ,  $1.0 \times 10^{-7}$  M  $\text{Na}_2\text{MoO}_4$ ,  $1.0 \times 10^{-8}$  M  $\text{Na}_2\text{SeO}_3$ , and  $5.0 \times 10^{-8}$  to  $5.0 \times 10^{-6}$  M  $\text{FeCl}_3$ . The medium was passed through a Chelex column and then microwave sterilized. All trace metals, EDTA, and  $\text{PO}_4$  were syringe filtered and added after microwave sterilization. Bacterial cultures were grown at room temperature on a platform shaker (109 rpm). Prior to each experiment, cultures were transferred three times through the iron-poor PC medium ( $5.0 \times 10^{-8}$  M) to ensure iron-limited growth (9). Iron limitation was confirmed in the final transfer by comparison to the growth of subcultures spiked with  $5.0 \times 10^{-7}$  M Fe at 20 h. Iron-added versus unamended replicate cultures were compared after 24 h of incubation with the added Fe spike.

**Growth on heme sources.** All iron stocks were syringe filtered prior to addition. The following Fe stocks were dissolved and stored at 4°C: Fe(III) chloride ( $\text{FeCl}_3$ ) in 0.1 M HCl; 5,10,15,20-tetraphenyl-21H,23H-porphine-p,p',p'',p'''-tetrasulfonic acid tetrasodium hydrate (TPP) in Milli-Q water (18 mM); ferrated 5,10,15,20-tetraphenyl-21H,23H-porphine-p,p',p'',p'''-tetrasulfonic acid tetrasodium hydrate (FeTPP) in methanol; hemoglobin A ferrous (Hb) in TAE (Tris-acetate-EDTA) buffer (pH 8.2) (see Fig. S1 in the supplemental material). Coproporphyrin (COP), Fe(III) coproporphyrin (FeCOP), protoporphyrin IX (PPIX), and hemin were all dissolved in methanol and stored at  $-20^\circ\text{C}$  (see Fig. S1). Bacterial cultures were grown at room temperature on a platform shaker (109 rpm). Prior to each growth experiment, cultures were transferred two times through the iron-poor PC medium (50 nM  $\text{FeCl}_3$ ) and then supplied with the iron sources on the third transfer into PC medium (no added Fe) and monitored for growth on a UV-VIS spectrophotometer at an optical density at 600 nm ( $\text{OD}_{600}$ ) for  $\sim 60$  h. Added Fe concentrations were 0 nM  $\text{FeCl}_3$  for the control and 500 nM  $\text{FeCl}_3$ , TTP, FeTTP, COP, FeCOP, PPIX, hemin, or Hb for the cultures with added Fe sources.

**Uptake of iron from heme.** Radioactive iron stocks were prepared from a stock solution of  $^{55}\text{FeCl}_3$  (82.68 mCi  $\text{mg}^{-1}$ ; PerkinElmer).  $^{55}\text{Fe}$ (III)-heme ( $^{55}\text{FePPIX}$ ) was synthesized following the procedure described in reference 15. Briefly,  $^{55}\text{FeCl}_3$  (25  $\mu\text{M}$ ) was refluxed with equimolar protoporphyrin IX in glacial acetic acid containing 0.1 M sodium acetate for 2 h (19). The glacial acetic acid solution was diluted to 50% strength with water and then passed through a column of Diaion HP20S resin. The column was washed with water, and the  $^{55}\text{FePPIX}$  was eluted in acetone. The concentration and purity of the  $^{55}\text{FePPIX}$  were determined by UV-Vis spectroscopy by comparison with purchased heme standards (Sigma) and added to experimental cultures at 5 nM  $^{55}\text{FePPIX}$ . Specific activity of the heme was determined by counting  $^{55}\text{Fe}$  in a Beckman LS6000IC scintillation counter as described below.

Iron-replete ( $5 \times 10^{-6}$  M) and iron-limited ( $5 \times 10^{-7}$  M) bacterial cultures were grown in PC medium and were harvested in exponential phase ( $\sim 20$  h of growth) by centrifugation at 9,000 rpm (8,784 relative centrifugal force) for 10 min at  $22^\circ\text{C}$  in a Heraeus 17 RS centrifuge. The bacteria were rinsed by centrifugation and resuspended three times with chelexed (20) artificial seawater ( $4.20 \times 10^{-1}$  M NaCl,  $2.88 \times 10^{-2}$  M  $\text{Na}_2\text{SO}_4$ ,  $9.39 \times 10^{-3}$  M KCl,  $2.38 \times 10^{-3}$  M  $\text{NaHCO}_3$ ,  $5.46 \times 10^{-2}$  M

$\text{MgCl}_2$ ,  $1.05 \times 10^{-2}$  M  $\text{CaCl}_2$ ). Final bacterial suspensions corresponded to an  $\text{OD}_{600}$  of 0.03 to 0.04 in Chelex-treated artificial seawater. Bacterial  $^{55}\text{FePPIX}$  uptake experiments were set up in triplicate live cultures, with one 0.01% glutaraldehyde-killed control. All cultures were incubated at room temperature in the dark. Measurements were taken at 25, 50, 75, 105, 135, and 165 min following addition of  $5 \times 10^{-9}$  M  $^{55}\text{FePPIX}$ . At each time point, 2 ml of bacteria was rapidly filtered ( $<12.7$  cm Hg) onto a 0.45- $\mu\text{m}$  membrane filter. The filter was sequentially rinsed with 5 ml of 0.2- $\mu\text{m}$ -filtered seawater, 2 ml of Ti-citrate wash (21) for 2 min to remove extracellular iron, and 5 ml of 0.2- $\mu\text{m}$ -filtered seawater. The filters were then placed in a scintillation vial with the scintillation cocktail Ecolite (MP), stored overnight, and counts were read on the scintillation counter. Microscopic cell counts were taken every hour from a nonradioactive culture of bacteria maintained identically to the radioactive cultures throughout the duration of the experiment and preserved in 1% glutaraldehyde. The samples were then filtered on a 0.2- $\mu\text{m}$  filter and stained with 4',6'-diamidino-2-phenylindole. All slides were made within 3 days of being collected and were counts were determined on an Olympus AX70 EPI fluorescence microscope. The bacteria in 10 random fields from each filter were counted (20% standard deviation). The  $^{55}\text{Fe}$  uptake per cell was corrected for any nonspecific FePPIX binding observed by subtracting  $^{55}\text{Fe}$  uptake in the glutaraldehyde-killed controls.

**Identification of heme systems in *Roseobacter* genomes.** The genome of *Ruegeria* sp. TrichCH4B was searched for potential heme uptake genes. The outer membrane receptor (HmuR) was identified with a hidden Markov model (HMM) created from functionally characterized heme transporters, using the HMMERv3.0 software suite (15, 22). The heme oxygenase and/or chaperone protein (HmuS) was identified by using Pfam HMM PF05171. The ExbD proteins were identified by Pfam HMM PF02472 (23). The ABC transporter (HmuTUV) components ExbB and TonB were identified by BLASTp searches (24) of the curated UniProtKB/Swiss-Prot database (25) through the NCBI BLAST servers.

The genomes of marine roseobacters in the RoseoBase database (<http://www.roseobase.org/>) were searched for the presence of heme uptake and utilization genes (March 2013). Identified heme proteins in *Ruegeria* sp. TrichCH4B were used to conduct a BLASTp search of the database.

**Gene expression.** TrichCH4B was grown on different concentrations of FePPIX or  $\text{FeCl}_3$  and harvested in exponential phase ( $\sim 20$  h) for analysis of gene expression. Prior to RNA extraction, cultures were transferred two times through iron-poor PC medium (50 nM  $\text{FeCl}_3$ ) and on the third transfer into PC medium (no Fe added) supplemented with  $\text{FeCl}_3$  (50 nM, 500 nM, or 5  $\mu\text{M}$ ) or hemin (500 nM). After  $\sim 20$  h of growth, cultures were harvested by centrifugation, and RNA was isolated with the TRIzol Max bacterial isolation kit (Invitrogen) following the manufacturer's instructions, with the exception of the cell lysis step, for which cells were incubated for 30 min at  $50^\circ\text{C}$  with TRIzol. The isolated RNA was purified with an RNeasy purification kit (Qiagen) and with amplification-grade DNase I (Invitrogen). The RNA was quantified based on the absorbance at 260 and 280 nm, measured on a NanoDrop spectrophotometer model ND-1000. Total RNA (500 ng) was reverse transcribed to produce cDNA with SuperScript III first-strand synthesis for real-time quantitative PCR (RT-Q-PCR; Invitrogen) following the manufacturer's instructions. RT-Q-PCR was performed on the cDNA to quantify relative transcript amounts by using a Stratagene Mx3000P with the Brilliant Sybr green Q-PCR master mix (Stratagene) and gene-specific primers (0.42  $\mu\text{M}$ ) (Table 1) designed using the draft genome of TrichCH4B. Temperature profiles for the Q-PCR consisted of an initial 10 min at  $95^\circ\text{C}$ , followed by 40 cycles of  $95^\circ\text{C}$  for 1 min, 30 s at an annealing temperature  $2^\circ\text{C}$  above the melting temperature of the primers ( $56^\circ\text{C}$ ), and 30 s at  $72^\circ\text{C}$ . To quantify the samples, a five-point standard curve of genomic DNA was analyzed for each gene, based on the crossing of a threshold fluorescence level chosen within the early range of exponential Q-PCR amplification. Genomic DNA was isolated from TrichCH4B cells grown in 1/10 SWC medium by using a DNeasy kit (Qiagen) and quantified on the spectrophotometer. Melting curve analysis, which followed the Q-PCR and initial screening of

TABLE 1 *Ruegeria* sp. TrichCH4B genes investigated by RT-Q-PCR and primers used for the analysis

Gene	Putative function	Accession no.	Forward primer	Reverse primer
<i>hmuV</i>	ABC ATPase	ZP_05740219.1	5'-GTCACCCTTGTGGCTGTTT	5'-GGGCAACCATAGACCTGAGA
<i>hmuU</i>	ABC permease	ZP_05740821.1	5'-CAGAGCCTCTTTGGCCATTA	5'-CACGCAGTTGATTGTCATCC
<i>hmuT</i>	ABC periplasmic binding protein	ZP_05740084.1	5'-ATCTATGCGCTTGGAGGAGA	5'-TTTCAGGACCTCAAGCGTCT
<i>hmuS</i>	Heme oxygenase/chaperone	ZP_05740627.1	5'-CGGATGTGATAGCGGAACCT	5'-TGACATGCGCTCTACAAAGG
<i>hmuR1</i>	TonB-dependent heme outer membrane receptor	ZP_05739888.1	5'-CGGACCAGTGGATTGAGAAT	5'-GTTGCCAAAGTCCATTTCTGT
<i>hmuR2</i>	TonB-dependent heme outer membrane receptor	ZP_05742350.1	5'-TCTGCGAATACTTCGTCGTG	5'-GTATGAGGTGCGTCGGAGGAA
<i>tonB</i>	TonB family protein	ZP_05740518.1	5'-ACCAACCTGACAAGGCAAG	5'-TACCAGCCCTGATAGTTGG
<i>exbB</i>	MotA/TolQ/ExbB proton channel	ZP_05740801.1	5'-TGTGTTGTTGATTGCCCTGT	5'-TATTGGATTGCGCCAAAAGT
<i>exbD1</i>	Biopolymer transport protein	ZP_05740215.1	5'-TCATGCTGTGTCACACATT	5'-CTCACCTGACAGGCTCAACA
<i>exbD1a</i>	Biopolymer transport protein	ZP_05740665.1	5'-GGCCTATGTGCGCATTAATCT	5'-TGACAGGTTTCGCTCTGACA
<i>rpoD</i>	RNA polymerase	ZP_05740285.1	5'-CGTCGCGGCTATAAGTTCTC	5'-CTTGGCGATTTTCATCACCT
	Hypothetical protein	ZP_05740288.1	5'-GAGGGTCAGGTGATGATGCT	5'-AGAGCAAAAGCCCTTCTGTG

PCR products by gel electrophoresis (1% agarose), verified that a single product of the expected length was amplified by each primer set. Parallel reactions were run without reverse transcriptase, and no products were formed during Q-PCR, indicating that there was no contaminating DNA. All gene expression levels were first normalized to that of the housekeeping gene *rpoD* (26, 27) and then compared to that of the Fe-replete ( $5 \mu\text{M FeCl}_3$ ) culture.

**Phylogenetic analyses.** The *Roseobacter* 16S rRNA phylogeny was constructed by aligning identified *Roseobacter* 16S rRNA sequences to the Greengenes ribosomal database by using PyNAST (28). RAxML v7.4.2 was used to generate a maximum likelihood tree under the gamma distribution, using the general time-reversible model for DNA evolution and utilizing 500 random sampling bootstraps (29). The HmuS reference phylogenetic tree was generated from an amino acid multiple sequence alignment of the full HmuS protein. Sequences were obtained by selecting the top 250 BLASTp hits to the full *Ruegeria* sp. TrichCH4B HmuS protein (accession number: ZP\_05740627) in the NCBI nonredundant protein database. These top hits comprised a diverse taxonomy, including *Alphaproteobacteria*, *Betaproteobacteria*, *Deltaproteobacteria*, and *Gammaproteobacteria*, *Bacteroidetes*, *Spirochaetes*, and *Acidobacteria*. The lowest-scoring hit showed coverage of 95%, a percent similarity of 40%, and an E value of  $5 \times 10^{-70}$ . To ensure inclusion of marine isolates not yet indexed in the NCBI database in the reference phylogeny, the TrichCH4B HmuS protein was searched against the Moore Microbial Genome Sequencing Project from the CAMERA database using BLASTp and an E value cutoff of  $10^{-50}$  (30). In total, 264 protein sequences from cultured isolates were aligned against the HMM PF05171 by using the HMMER v3.0 software suite (22), and a reference maximum likelihood phylogenetic tree was constructed in RAxML v7.4.2 under the gamma distribution and utilizing the Whelan and Goldman amino acid substitution matrix (29, 31). The robustness of inference of the tree was assessed by using 250 random sampling bootstraps. For the phylogenetic analysis of environmental *hmuS* sequences (see next section), the translated sequence fragments were added to the full-length HmuS reference tree alignment by using HMMER v3.0, and the pplacer v1.1 alpha13 software suite was used to place those sequence fragments on the fixed topology of that reference tree. An unrooted informative subset of the global tree topology was selected by using the guppy “trim” command. Edges to which amplicons mapped with maximum likelihood are denoted with a pie chart proportional in size to the total number of sequences mapping there and showing the sampling categorization of the sequences (32). This information is also available in tabular format in Table S1 of the supplemental material. All trees were viewed with the Archaeopteryx tree viewer (33).

**DNA isolation from the environment.** Seawater samples were collected from the Kendall-Frost Reserve in San Diego, CA, in July 2011; from the San Dieguito Lagoon in Del Mar, CA, in January 2011; and from the California Current Ecosystem Long Term Ecological Research site (LTER) June/July 2011 cruise in the southern part of the California cur-

rent. Samples from two LTER stations were used. LTER station 1 was farther north (lat 34.09, long  $-121.61$ ) with samples collected at 2 m, the chlorophyll maximum at 39 m, and 81 m. LTER station 2 (lat 33.52, long  $-121.12$ ) had higher surface chlorophyll values, and samples were collected at 5 m, the chlorophyll maximum at 25 m, and 100 m. The volume of filtered seawater ranged from 500 ml to 1 liter, depending on the amount of biomass in the water. Seawater was filtered onto a  $0.2\text{-}\mu\text{m}$  Supor filter (Pall) and stored at  $-80^\circ\text{C}$  until DNA isolation. The DNA was isolated following the procedure described in reference 34. The DNA was quantified based on the absorbance at 260 and 280 nm as measured on a NanoDrop spectrophotometer model ND-1000.

**Detecting environmental *hmuS* gene sequences.** Eight *Alphaproteobacteria* heme oxygenase and/or chaperone gene sequences were aligned by using ClustalX 2.0.12 (35) to find conserved regions of the gene (see Fig. S2 in the supplemental material). The *hmuS* gene was selected for degenerate primer design since it is relatively well conserved compared to other genes in the heme uptake system. A degenerate *hmuS* primer set, forward primer 5'-GAGGTBATGGCCTVACSCG and reverse primer 5'-CANGCRTSCCCSGCNGC, was designed to amplify a 450-bp section of the gene. The *hmuS* degenerate primers had 36- and 192-fold degeneracy in the forward and reverse primers, respectively. The primers were tested on a selection of cultured *Proteobacteria* and *Bacteroidaceae* and were specific for *Alphaproteobacteria* (data not shown). The environmental DNA was amplified using the degenerate primers and touchdown PCR with temperature profiles of 1.5 min at  $94^\circ\text{C}$ , followed by 13 cycles of 30 s at  $94^\circ\text{C}$ , and 30 s at  $63^\circ\text{C}$  with a temperature increment of  $-1^\circ\text{C s}^{-1}$  and ramp of  $3^\circ\text{C}$ , 1 min at  $72^\circ\text{C}$ , followed by 27 cycles of 30 s at  $94^\circ\text{C}$ , 30 s at  $55^\circ\text{C}$ , and 1 min at  $72^\circ\text{C}$ , followed by 15 min at  $72^\circ\text{C}$ . A band 450 bp long was identified on gel electrophoresis and cut from the gel with a Zymo-clean Gel DNA kit (Zymo). The PCR product was used for cloning, following the manufacturer's instructions for the TOPO TA cloning kit (Invitrogen) with One Shot TOP10 chemically competent cells. Twenty clones were selected from each environmental sample, and the cloned product was retrieved using the Qiagen spin miniprep kit following the manufacturer's instructions. The plasmid was sequenced by Retrogen, San Diego, CA, and sequence traces were analyzed using Sequencher 5.0 (Gene Codes Corporation) and identified as *hmuS* using BLASTx against the NCBI nonredundant protein database. The degenerate primers may need to be redesigned in the future, as  $\sim 70\%$  of the cloned sequences were identified as hypothetical, pyruvate kinase, or D-3-phosphoglycerate dehydrogenase genes and did not represent *hmuS* genes; also, they were not specific to the *Roseobacter* clade. Additionally, the Global Ocean Sampling Combined Assembly Proteins database in CAMERA was searched using the TrichCH4B HmuS protein, with an E value cutoff of  $10^{-10}$ , and this produced 20 hits each with at least one occurrence of the HmuS-ChuX domain from PF05171. The assemblies were derived from sequenced DNA pooled from the 52 samples of the GOS expedition leg described by Rusch et al. (36).

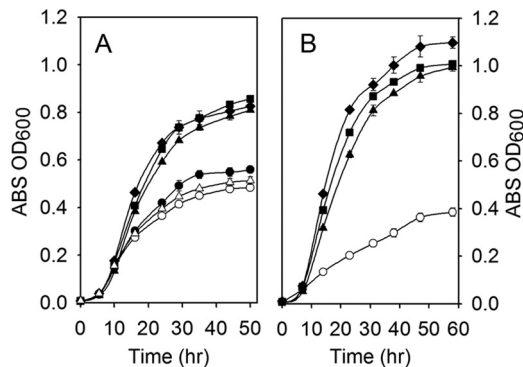


**FIG 1** *Ruegeria* sp. TrichCH4B growth on various iron sources. (A) Growth on 0 nM FeCl<sub>3</sub> (open circles), 500 nM FeCl<sub>3</sub> (filled squares), 500 nM FePPIX (filled triangles), 500 nM FeCOP (filled diamonds), 500 nM FeTTP (filled circles), and 500 nM porphyrin (average of PPIX, COP, and TTP growth; open triangles). (B) Growth on 0 nM FeCl<sub>3</sub> (open circles), 500 nM FeCl<sub>3</sub> (filled squares), 500 nM FePPIX (filled triangles), and 500 nM Hb (filled diamonds). All treatments were performed in duplicate, and error bars are standard deviations of the means. Most error bars are within the size of the symbol.

**Data analysis.** A paired two-tailed *t* test was used to compare the radiolabeled [<sup>55</sup>Fe]heme uptake levels between the Fe-replete and Fe-deplete cultures. A second set of *t* tests was used to compare the gene expression levels of the heme uptake and utilization system when grown on varied amounts of Fe and different Fe sources. The *t* test was completed with commercially available software in Excel. For all *t* tests, the 95% confidence level was used to determine statistical differences.

**Nucleotide sequence accession numbers.** The original sequences obtained in this study were deposited in the GenBank database under sequence accession numbers [JX081594](#) to [JX081598](#) and [JX081600](#) to [JX081644](#).

## RESULTS

**Growth on heme sources.** Iron-limited *Ruegeria* sp. TrichCH4B was grown in the presence of the porphyrin molecules PPIX, COP, and TPP (see Fig. S1 in the supplemental material for structures), in both apo- and Fe-complexed forms, for 50 h (Fig. 1A). The substantial growth of TrichCH4B on FeCOP and FePPIX was very similar, with a maximum OD of ~0.8 at 50 h. The observed growth yield on these sources was nearly identical to that on inorganic FeCl<sub>3</sub>, and the shapes of the growth curves for these Fe sources were identical. In contrast, TrichCH4B showed significantly less growth on FeTTP than on inorganic FeCl<sub>3</sub>. FeTTP is a synthetic compound with phenyl side groups attached to the bridging carbons on the porphyrin ring, which makes it presumably more difficult to transport than the natural heme sources FePPIX and FeCOP, due to steric effects (see Fig. S1). Lack of growth on FeTTP compared to other heme sources implicates heme transport, not Fe extraction, as the Fe acquisition mechanism, although the potential for steric hindrance of an external iron extraction molecule by the phenyl groups cannot be ruled out by these data. The growth of TrichCH4B on the porphyrin sources (PPIX, COP, and TPP) without Fe was similar to the growth of the control culture without added porphyrin or iron, signifying that the Fe-free porphyrins are not beneficial for growth under iron-limiting conditions. A second growth experiment (Fig. 1B) was conducted with a large hemoprotein, hemoglobin, as the iron source. The growth rate on hemoglobin was faster and yielded a greater final OD than growth on inorganic FeCl<sub>3</sub> or FePPIX. The

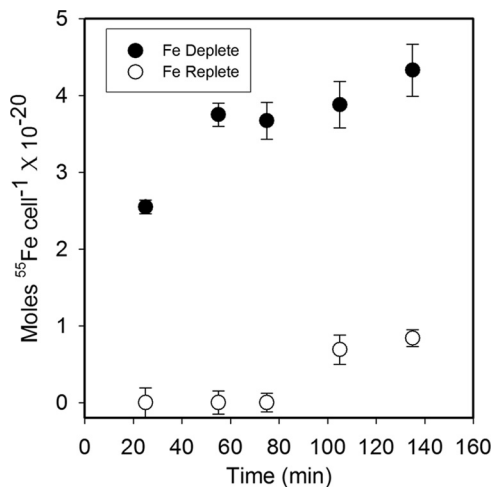


**FIG 2** Uptake of radiolabeled FePPIX. The intracellular accumulation of <sup>55</sup>Fe from FePPIX is shown over 3 h of incubation. Depleted cultures contained 50 nM FeCl<sub>3</sub>, and replete cultures contained 5 μM FeCl<sub>3</sub>. All measurements were from triplicate cultures, and error bars are standard deviations of the means.

final OD of the culture grown on hemoglobin was 1.1 times greater than the final OD of the inorganic FeCl<sub>3</sub> and FePPIX cultures (Fig. 1B). The second growth experiment produced slightly higher final ODs on inorganic FeCl<sub>3</sub> and FePPIX cultures than the first experiment, which may have been due to slight differences in the degree of iron limitation of the inoculating cultures.

**Radiolabeled heme uptake.** The intracellular uptake of Fe from <sup>55</sup>FePPIX could be quantified and observed in both Fe-replete (5 μM Fe) and Fe-depleted (50 nM Fe) TrichCH4B cultures (Fig. 2). The ability of TrichCH4B to acquire Fe from FePPIX was directly related to the degree of Fe limitation, with <sup>55</sup>Fe uptake in the Fe-depleted culture roughly 4 times greater than that under Fe-replete conditions (*P* < 0.05). The acquisition of Fe from FePPIX was rapid in the Fe-depleted culture, with the majority of the uptake occurring during the first hour of incubation, whereas the uptake in the Fe-replete culture was slow and occurred later in the experiment.

**Gene identification.** A complete heme uptake system was identified in two apparent operons that are adjacent in the genome of TrichCH4B but transcribed in opposite directions (Fig. 3). The organization of one of the operons consisted of the putative ABC transporter components (*hmuTUV*) and the putative heme oxygenase and/or chaperone (*hmuS*) gene. The second operon consisted of the putative outer membrane receptor (*hmuR1*) and putative TonB components (*exbBD tonB*). Within the second operon, an unidentified hypothetical protein and a second *exbD* gene (*exbD1a*) were identified. Although both *exbD* genes were identified based on the *exbD* Pfam HMM (PF02472), the *exbD1a* gene had lower hit values (score, 40; E value,  $1.8 \times 10^{-10}$ ) than *exbD1* (score, 64; E value,  $6.8 \times 10^{-18}$ ) to this Pfam. The two ExbD proteins had few similarities (query coverage of 27%; 34% identity and 622% similarity) to each other based on a BLASTp analysis. Both *exbD* genes had a GC content (58% and 61%) similar to the genome GC content of 59%, suggesting that the *exbD* genes were not recently acquired through horizontal gene transfer. A second set of *exbD* genes was identified in the genome next to siderophore components, which have similar properties to the heme *exbD*, and this also suggested that these genes are not the result of a recent duplication event. A second *hmuR* gene (*hmuR2*)

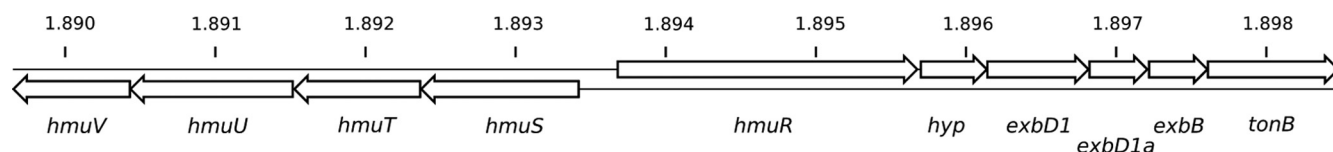


FIG 3 Genomic organization of the heme system in *Ruegeria* sp. TrichCH4B. *hyp*, hypothetical protein. Numbers are  $10^6$  bp and represent the position in the *Ruegeria* sp. TrichCH4B genome.

was found in the genome, but it was not in an operon or next to any TonB components. All of the protein sequences of the heme uptake system in TrichCH4B had hits to known functional heme proteins in the UniProtKB/Swiss-Prot database (see Table S2 in the supplemental material). The protein sequences from TrichCH4B showed greater-than-37% identity to known heme proteins in pathogenic bacteria. The weakest hit (21% identity) was to the outer membrane receptor, which has been shown to be divergent in marine organisms (15).

**Gene expression.** The previously identified heme uptake system of TrichCH4B (Fig. 3) was investigated for gene expression under four different Fe treatments: 50 nM FeCl<sub>3</sub>, 500 nM FeCl<sub>3</sub>, 5 μM FeCl<sub>3</sub>, and 500 nM FePPIX, to investigate how Fe limitation affects gene expression of the heme uptake system. Under Fe-limiting conditions (50 nM FeCl<sub>3</sub>) all of the genes in the heme uptake system were highly upregulated, with expression levels 100 to 1,000 times higher for the Fe-replete culture (5 μM) (Fig. 4) at levels statistically significant ( $P < 0.05$ ) for all genes except *exbD1*. Under Fe stress conditions (500 nM FeCl<sub>3</sub>), all of the genes continued to be upregulated at expression levels 5 to 10 times higher than in the Fe-replete culture (statistically significant [ $P < 0.05$ ] for all genes). When TrichCH4B was grown on 500 nM FePPIX (heme), the level of gene expression was very similar to that for the culture grown on 500 nM FeCl<sub>3</sub>, and upregulation was statistically significant ( $P < 0.05$ ) for all genes except *exbB*. However, there were notable differences in the level of expression of the outer membrane receptor (*hmuR1*) and the TonB complex components when grown on FePPIX compared to FeCl<sub>3</sub>. The expression of the outer membrane receptor (*hmuR1*) when grown on FePPIX was

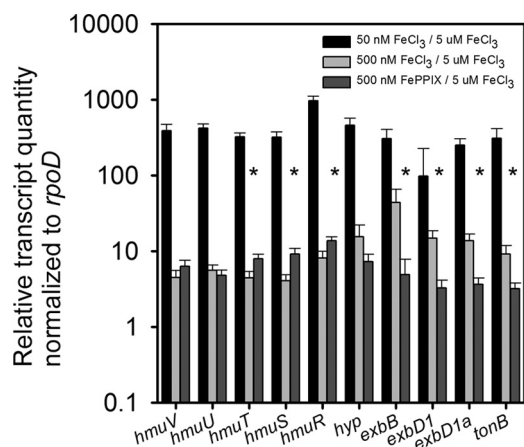
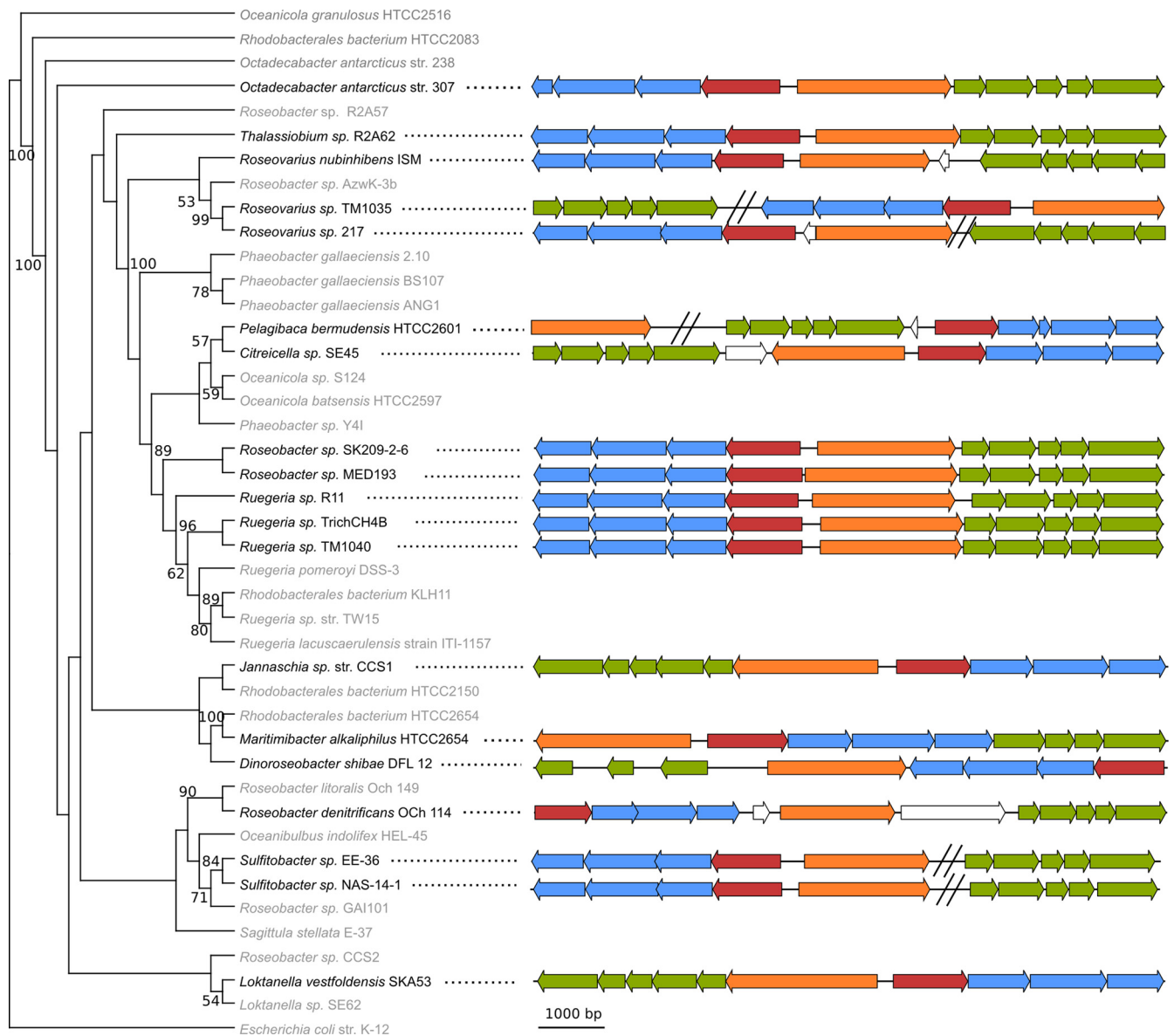


FIG 4 Gene expression of *Ruegeria* sp. TrichCH4B grown on various Fe sources. All gene expression levels were first normalized to the housekeeping gene *rpoD* and then normalized to the Fe-replete (5 μM Fe) expression levels. All gene expression values were from triplicate measurements, and error bars are standard deviations of the means. \*, statistically different expression levels between the 500 nM FeCl<sub>3</sub> and 500 nM heme groups ( $P < 0.05$ ).

statistically greater ( $P < 0.05$ ) than for the culture grown on similar amounts of FeCl<sub>3</sub> (Fig. 4). The TonB complex components were expressed significantly less ( $P < 0.05$ ) when grown on FePPIX than with the culture grown on similar amounts of FeCl<sub>3</sub> (Fig. 4). The second outer membrane receptor (*hmuR2*) showed increased gene expression in response to Fe scarcity, with levels 7 to 34 times higher than the Fe-replete culture, with the 50 nM FeCl<sub>3</sub> culture being expressed at least twice as high as the 500 nM FeCl<sub>3</sub> culture and nearly five times as much as the 500 nM heme culture (data not shown). The observed inverse correlation between heme uptake gene expression and the inorganic Fe concentration, as well as the variations in heme receptor expression depending on the Fe source, suggest that TrichCH4B responds to dynamic Fe availability in its immediate environment through specific transcriptional responses of its Fe uptake capabilities.

**Heme systems in other *Roseobacter* clade isolates.** The genomes of various marine roseobacters in the RoseoBase database were investigated for the presence of heme uptake systems by searching with the heme proteins identified in the genome of TrichCH4B. Of the 45 genomically sequenced strains in the database, approximately half, 19 of 45, of the bacteria had complete heme uptake systems (see Table S3 in the supplemental material). The majority of these (13 strains) had all of the identified heme uptake genes of TrichCH4B, and these genes were generally organized similarly, often in two adjacent operons, as in TrichCH4B (Fig. 5). The remainder of the bacteria had the heme uptake system spread out in the genome, with the heme transport genes (*hmuRSTUV*) typically clustering together and the TonB complex genes clustering together (Fig. 5). A common feature in nearly all of the bacterial heme systems is the presence of the hypothetical protein and two ExbD proteins within the TonB complex cluster. Within each set of roseobacter ExbD proteins, one protein had a better match score to the Pfam HMM (PF002472) (data not shown), and each ExbD matched well to only one of the TrichCH4B ExbD proteins (see Table S4 in the supplemental material).

**Detection of environmental *hmuS* genes.** Various samples from marsh (Kendall-Frost Reserve, San Diego, CA, and San Dieguito Lagoon, Del Mar, CA) and pelagic ocean (California Current Ecosystem LTER site) environments were screened for the *Roseobacter* clade heme oxygenase and/or chaperone gene. *HmuS* is the most genetically conserved component in the putative heme utilization operon identified in members of the *Roseobacter* clade, and the degenerate primer set was designed using only *Roseobacter hmuS* sequences. Marine *Gammaproteobacteria* have a homologous gene, *hutX*, but it is unlikely that this gene would be amplified, since the *hmuS* degenerate primer set does not match well to the *hutX* gene sequences (~50% of the degenerate primer nucleotides match). The gene *hutZ* in *Vibrio cholerae* appears to perform a similar function as *hmuS* (32), but its genes are not homologs (BLASTp query of 39%, 25% identity and 44%



**FIG 5** A 16S rRNA maximum likelihood phylogeny from the 43 *Roseobacter* genomes indexed in RoseoBase that had an identifiable and complete 16S rRNA sequence. *Escherichia coli* strain K-12 was used as an outgroup, and bootstrap values of >50% are shown for 500 resamplings. The tree is visualized without informative branch lengths for simplicity. *Roseobacter*s with a complete heme uptake system are shown in bold black, with a genome schematic of their respective heme uptake region. Bar, approximate size of 1,000 bp of DNA; colors designate functional categories within the apparent heme uptake operon. The ABC ATPase, permease, and substrate binding proteins are shown in blue, the heme oxygenase (*hmuS*) is shown in red, and the outer membrane receptor (*hmuR*) is shown in orange. Components of the putative TonB energy transduction complex (including the conserved hypothetical protein) are in green, while any other nonconserved hypothetical proteins are in white. Hash marks indicate separations in the genome of greater than 10 kb. See Table S3 in the supplemental material for protein accession numbers for the translated product of each gene.

similarity), and *hutZ* should not be detected with the *hmuS* degenerate primer set. Confirmation of the specificity of the *hmuS* degenerate primer set to *Alphaproteobacteria* was observed for a number of laboratory isolates (described in Materials and Methods). Once cloned, all of the environmental amplicons were evaluated by using BLASTx against the NCBI nonredundant database, and genes identified as *hmuS* were detected in every sample and only belonged to the *Roseobacter* clade. The environmental sequences that were identified as *hmuS* had top BLASTx hits to marine *Alphaproteobacteria* HmuS proteins and appeared to have

the correct amino acids for heme binding (see Fig. S3 and Table S5 in the supplemental material).

A total of 51 *hmuS* sequences were identified from the marsh and pelagic ocean environments. Of these, 39 sequences were identified from the pelagic ocean samples, with 28 sequences obtained from the surface-to-chlorophyll maximum samples and 11 sequences obtained at depths below the chlorophyll maximum. At LTER station 2, characterized by a large diatom bloom with a chlorophyll maximum at 25 m, half of the *hmuS* sequences obtained from this station were from the chlorophyll maximum. At

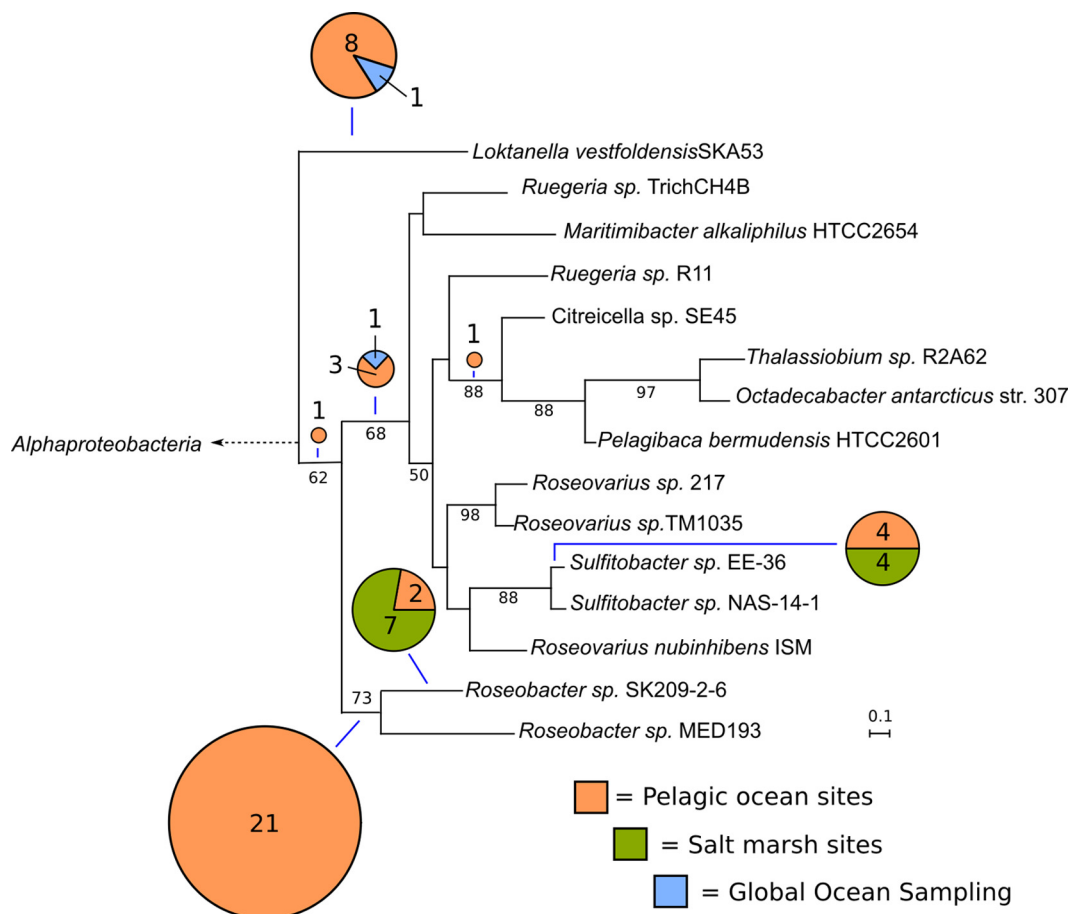


**FIG 6** Phylogenetic tree of translated HmuS environmental fragments mapped to the topology of the 264 full-length HmuS sequence maximum likelihood phylogeny. The portion visualized is an unrooted subset of the *Rhodobacteraceae* family, which is equivalent to the *Rhodobacteraceae* designated in Fig. S4 in the supplemental material, and the dashed arrow points to the encompassing *Alphaproteobacteria* clade. Robustness of inference was assessed by using 250 random sampling bootstraps, and support values greater than 50 are displayed. The scale bar indicates the distances in substitutions per site. Edges to which environmental fragments mapped with maximum likelihood are designated by blue lines pointing to a pie chart, proportional in size to the number of queries placed there. The pie charts are broken-down by sample category, with pelagic ocean sites within the California current shown in orange, salt marsh sites shown in green, and GOS sequences in blue. Numbers inside or pointing to pie charts regions indicate the numbers of queries.

LTER station 1, characterized by lower chlorophyll concentrations and a less distinct and deeper chlorophyll maximum, the opposite trend was observed, with more sequences obtained from above and below the chlorophyll maximum.

We examined the taxonomic classification of the *hmuS* amplicons in further detail by using pplacer's short read mapping algorithm. Whereas BLAST can infer taxonomy of a given sequence by a "best hit" pairwise similarity to a database, pplacer can classify unknown sequences by adding them to a fixed, previously determined phylogeny where the taxonomic structure is assumed to be known. The pplacer approach has the added advantage of incorporating the underlying statistical and evolutionary models of the reference phylogeny into the classification procedure. Briefly, the pplacer algorithm finds an attachment location and pendant branch length for a given query sequence in the reference phylogeny that maximizes the likelihood of the resulting tree without altering the structure of the original reference phylogeny. The query sequence is classified at a taxonomic rank from a node in the tree that has both the query sequence and flanking branches as a common descendant. In our reference tree we included full-length HmuS sequences from a diverse microbial tax-

onomy (see Materials and Methods) to see if our cloned environmental sequences reliably mapped to the *Roseobacter* clade in the context of the overall phylogeny of the translated gene. Fig. S4 of the supplemental material shows the global maximum likelihood tree topology, with the *Roseobacter* clade highlighted in a black box. In this phylogeny, the marine *Roseobacter* groups within a larger cluster of *Alphaproteobacteria*, which are highlighted with a gray background. This clade branches away from the rest of the proteobacteria relatively early in the phylogeny. Marine *Gammaproteobacteria* HutX sequences are located deeper within the tree but have bootstrap support below 50. Thus, it is unclear as to the exact evolutionary relationship between the marine *Gammaproteobacteria* and *Alphaproteobacteria* heme oxygenases, but the two groups are different enough to warrant their separation in the phylogeny. Given the distinctness of the *Roseobacter* clade in the global heme oxygenase phylogeny and the robust amplicon recruitment to that clade, we believe that the cloned environmental *hmuS* sequences are from marine roseobacters. By extension, we assume our degenerate primer set is specific for the marine *Roseobacter* clade.

Figure 6 shows a subset of the reference *hmuS* phylogeny

(bootstrap values visualized), with environmentally derived sequences placed on the tree. Environmental amplicons could confidently be mapped to either family or genus taxonomic rank, with the majority of reads being annotated at the family level (see Table S1 in the supplemental material). There is a relatively large edge uncertainty for many of the reads, but the expected distances between placement locations (EDPL) are small. Thus, while there may be uncertainty in the amplicon placement within the *Roseobacter* clade, the uncertainty for global placement in the tree is low (37). The marsh samples were distributed into two groups, with one group clustering with *Sulfitobacter* sp. EE-36 and the other group clustering with *Roseobacter* sp. SK209-2-6. Sequences from the pelagic ocean samples were more widely distributed in the tree. The majority, 63%, of the pelagic ocean sequences were identified deep within the tree, suggesting that many of these sequences are not well represented among cultured organisms.

To place our results in a context with other metagenomic studies, the GOS metagenomic assemblies were searched for the presence of the HmuS ChuX domain (36). In total, 20 hits matching the HmuS ChuX domain were detected in the assemblies. Biers and colleagues previously estimated the total number of genome equivalents in the GOS data set at 4,045 (38). This abundance estimate suggests that the HmuS ChuX domain is present in fewer than 0.5% of the genomes sampled in GOS. Nonetheless, the phylogenetic analysis of the 20 GOS sequences can provide insight, albeit limited, as to how broadly this capability is distributed taxonomically in the marine environment. HmuS sequences from the GOS metagenomes mapped to a diverse taxonomic ranks, with the majority of reads only confidently mapping to the phylum, class, and family levels (see Table S1 in the supplemental material). Again, there was considerable uncertainty of the optimal placement for many of the reads, but global uncertainty (EDPL) was low. The low level of taxonomic resolution for many of the GOS sequences suggests that, at this point, sequenced strains with the HmuS ChuX domain rather poorly represent the overall diversity of the gene in the marine environment. Only 2 of the 20 metagenomic *hmuS* sequences mapped to *Alphaproteobacteria*, with the majority placed within *Gamma*proteobacteria. Interestingly, the two *Alphaproteobacteria* sequences were confidently resolved at the family rank of *Rhodobacteracea* in the *Roseobacter* clade (Fig. 6).

## DISCUSSION

The genome of TrichCH4B has a complete set of clustered heme uptake genes, based on gene identification by BLASTx analysis and comparison to known heme genes in previously characterized bacteria in the UniProtKB/Swiss-Prot database. At least four lines of evidence suggest that a heme system is functional in strain TrichCH4B. First, various natural heme sources, including FePPIX, FeCOP, and Hb, stimulated the growth of this organism and could replace FeCl<sub>3</sub> as an iron source. Second, TrichCH4B incorporated radiolabeled Fe from FePPIX. Third, expression of the putative heme uptake and utilization genes was inversely correlated to the Fe concentration. Fourth, 500 nM FeCl<sub>3</sub> or 500 nM FePPIX yielded similar degrees of relief from Fe stress, as measured by gene expression. Taken together, these results indicate that strain TrichCH4B can transport and utilize various natural heme compounds.

*Microscilla marina* and *Vibrio fischeri* are the only other non-pathogenic marine isolates thus far shown to utilize heme com-

pounds for growth, and of these, only *M. marina* is not host associated (15, 16). The potential use of heme as an iron source may be widespread among marine microbes, as the outer membrane receptor (*hmuR*) for heme uptake has been detected in the genomes of diverse marine bacteria and marine metagenomic data sets (15, 39). Thus, the data presented for TrichCH4B support the contention that heme may be a more important iron source in the marine environment than previously thought. Furthermore, our data for nine heme uptake and utilization genes in 19 *Roseobacter* clade isolates (Fig. 5; see also Table S3 in the supplemental material) and the detection of the heme oxygenase and/or chaperone gene (*hmuS*) in environmental samples (Fig. 6) both provide additional evidence that marine bacteria have the potential to utilize heme-type iron sources.

The heme uptake and utilization genes in the *Roseobacter* clade isolates have two common features that are present in nearly all of the isolates: the presence of a hypothetical protein, and the existence of two ExbD proteins (ExbD1 and ExbD1a) within the TonB complex cluster (see Table S3 in the supplemental material). The roles of the hypothetical protein and two ExbD proteins in heme acquisition by the *Roseobacter* clade are currently unknown. These extra proteins are not typically found in most functional heme systems in pathogenic bacteria (8, 15). However, there are a few documented occasions where heme uptake systems have additional proteins. Many *Vibrio* spp. have an extra protein of unknown function associated with the TonB complex, and in some this protein is essential for a functional TonB system (40), but this protein is not homologous (based on BLASTp analysis) to the TrichCH4B hypothetical protein. The presence of two *exbD* genes has thus far only been identified in the literature in two bacteria, *Xanthomonas campestris* pv. *campestris* (41, 42) and *Flavobacterium psychrophilum* (43). These TonB systems are believed to be associated with siderophore uptake systems in both of these bacteria, although heme uptake has not been investigated. In *Xanthomonas campestris* pv. *campestris*, one *exbD* gene cannot substitute for the other *exbD* gene during ferric iron acquisition, and it was proposed that the second *exbD* gene might broaden the scope of the TonB system (41, 42). This speculation may have some merit in the *Roseobacter* clade as well, since siderophore and/or heme uptake components were found adjacent to the *exbBD tonB* gene complex (see Table S6 in the supplemental material).

Heme utilization by members of the *Roseobacter* clade does not appear to be specific to one type of environment, as environmental *hmuS* sequences and (presumably) heme uptake-capable *Roseobacter* clade isolates have been detected/isolated in diverse habitats (seaweed, dinoflagellates, marsh, surface coastal, surface open ocean, deep ocean, and Antarctic waters). In addition to a global distribution, the *Roseobacter* clade shows no obvious 16S rRNA phylogenetic relationship between the isolates that potentially have heme uptake capability and those that do not (Fig. 5), suggesting that heme uptake is prevalent but somewhat unpredictably distributed throughout the *Roseobacter* clade.

The abundance of roseobacters in the ocean has been positively correlated with the abundance of phytoplankton (44–46). In this investigation, *hmuS* environmental sequences were most frequently detected in pelagic ocean surface waters and at the pelagic ocean chlorophyll maximum, where phytoplankton biomass was highest. This distribution of *hmuS* genes in the present study is consistent with other measurements of heme in the ocean, where the heme concentration has been positively correlated with chlo-



rophyll (13). Thus, it seems plausible that a link exists between the abundance of *Roseobacter hmuS* genes and phytoplankton-derived heme in the marine environment, although our data set at present is too limited to corroborate this claim.

We estimate that *hmuS* sequences are present in less than 0.5% of the genomes sampled in GOS. However, this is not particularly surprising, considering that the metagenomes are numerically dominated by *Prochlorococcus* spp. and *Pelagibacter ubique*, which lack any known component of heme uptake pathways (36, 39). In addition, it is still unclear to what degree the prevalence of *hmuS* genes is coupled to the abundance of heme outer membrane receptors in the environment. It has been estimated that approximately 10% of bacterial genomes in the GOS data set have HmuR-like outer membrane receptors for heme (39), while a separate study suggested that less than 1% of the marine bacterial population sampled in GOS maintains this Fe uptake capability (47). The great sequence diversity of TonB-dependent outer membrane receptors and increasing discoveries of new substrates (48) make functional prediction using TonB-dependent receptor sequence similarity alone challenging. Additionally, ambiguities in substrate assignment resulting from different methodologies between studies complicate the estimation of the prevalence of specific uptake pathways in environmental metagenomes. Future shotgun metagenomic studies targeting niches in the marine environment where heme uptake may be a more viable iron acquisition strategy (e.g., particle fractions or the phycosphere) will likely provide a broader phylogenetic/taxonomic context for examination of heme oxygenase/chaperone and heme outer membrane receptor genes from the marine environment (15, 49).

In conclusion, the model *Roseobacter*, *Ruegeria* sp. TrichCH4B, and potentially many members of the marine *Roseobacter* clade are capable of utilizing natural exogenous heme-type iron sources. These heme-type iron sources include small molecules, ferric protoporphyrin IX, and ferric coproporphyrin, as well as large hemoproteins, such as hemoglobin. This capability and the detection of *Roseobacter hmuS* genes in diverse marine habitats suggest that heme utilization in the marine environment may be more common than originally thought, and heme should be considered a bioavailable form of iron for free-living marine bacteria.

The consideration of heme as a bioavailable form of iron for bacteria in the marine environment suggests that direct heme uptake may be a viable pathway for iron recycling in the ocean. Nearly every organism utilizes heme as an intracellular iron binding molecule; thus, each organism has the potential to be a source of heme to the external environment upon cell lysis. The findings of this study indicate that many natural heme sources, ranging from small molecules to large hemoproteins, are bioavailable to bacteria, and it appears that the iron-porphyrin complex is taken up as a whole, as suggested by bacterial growth on various heme sources and the rapid uptake of heme under iron-limited conditions. The ability of bacteria to take up this well-defined iron chelate without alteration by produced ligands (e.g., siderophores) suggests that relatively refractory intracellular iron pools released with fresh intracellular material could be taken up quickly and directly reincorporated into living bacteria without previous degradation or the necessity of a siderophore intermediate. This evolving picture of iron cycling in marine systems contrasts with the accepted view, in which dissolved iron has generally been emphasized as the important iron pool available to marine microorganisms for uptake (50, 51), while the iron contained in intracel-

lular material and other organic particles has been considered bioavailable only after some sort of degradation or removal of iron from these materials, potentially by the use of siderophores (51, 52). While oceanic iron cycling is likely influenced by the ability of marine microbes to produce siderophores in organic-rich environments (53), direct heme transport should also be considered a viable iron acquisition strategy for non-host-associated planktonic marine microorganisms, consistent with the known ability of these microbes to attack organic matter in order to liberate nutrients for consumption (54, 55).

## ACKNOWLEDGMENTS

This work was funded by NSF graduate research fellowship grant DGE-1144086 to S.L.H., NSF grant OCE-0327070 to K.A.B. and Margo Haygood, and by NSF grant OCE-1061068 to K.A.B. and Bianca Brahamsha.

We thank the Palenik and Brahamsha labs for providing knowledge and lab space to carry out the gene expression and cloning work. We thank Ross Castillo, Tara Howell, and Maureen Quessenberry for their assistance with the environmental cloning work. We thank CCE-LTER for collection of the oceanic field samples. We thank Bianca Brahamsha, Margo Haygood, Elizabeth Mann, and Dorothy Parker for helpful discussion and review of the manuscript.

## REFERENCES

- Gledhill M, Van Den Berg CMG. 1994. Determination of complexation of Fe(III) with natural organic complexing ligands in seawater using cathodic stripping voltammetry. *Mar. Chem.* 47:41–54.
- Rue EL, Bruland KW. 1995. Complexation of iron(III) by natural organic-ligands in the Central North Pacific as determined by a new competitive ligand equilibration/adsorptive cathodic stripping voltammetric method. *Mar. Chem.* 50:117–138.
- Wu JF, Luther GW. 1995. Complexation of Fe(III) by natural organic-ligands in the Northwest Atlantic Ocean by competitive ligand equilibration method and a kinetic approach. *Mar. Chem.* 50:159–177.
- Buck KN, Bruland KW. 2007. The physicochemical speciation of dissolved iron in the Bering Sea, Alaska. *Limnol. Oceanogr.* 52:1800–1808.
- Hutchins DA, Witter AE, Butler A, Luther GW. 1999. Competition among marine phytoplankton for different chelated iron species. *Nature* 400:858–861.
- Weaver RS, Kirchner DL, Hutchins DA. 2003. Utilization of iron/organic ligand complexes by marine bacterioplankton. *Aquat. Microb. Ecol.* 31:227–239.
- Armstrong E, Granger J, Mann EL, Price NM. 2004. Outer-membrane siderophore receptors of heterotrophic oceanic bacteria. *Limnol. Oceanogr.* 49:579–587.
- Wandersman C, Delepelaire P. 2004. Bacterial iron sources: from siderophores to hemophores. *Annu. Rev. Microbiol.* 58:611–647.
- Roe KL, Barbeau K, Mann EL, Haygood MG. 2012. Acquisition of iron by *Trichodesmium* and associated bacteria in culture. *Environ. Microbiol.* 14:1681–1695.
- Chapman SK, Daff S, Munro AW. 1997. Heme: the most versatile redox centre in biology? *Metal Sites Proteins Models* 88:39–70.
- Strzepek RF, Harrison PJ. 2004. Photosynthetic architecture differs in coastal and oceanic diatoms. *Nature* 431:689–692.
- Gledhill M. 2007. The determination of heme b in marine phyto- and bacterioplankton. *Mar. Chem.* 103:393–403.
- Honey DJ, Gledhill M, Bibby TS, Legiret FE, Pratt NJ, Hickman A, Lawson T, Achterberg EP. 2013. Heme b in marine phytoplankton and particulate material from the North Atlantic Ocean. *Mar. Ecol. Prog. Ser.* 483:1–17.
- Vong L, Laes A, Blain S. 2007. Determination of iron-porphyrin-like complexes at nanomolar levels in seawater. *Anal. Chim. Acta* 588:237–244.
- Hopkinson BM, Roe KL, Barbeau KA. 2008. Heme uptake by *Microscilla marina* and evidence for heme uptake systems in the genomes of diverse marine bacteria. *Appl. Environ. Microbiol.* 74:6263–6270.
- Septer AN, Wang YL, Ruby EG, Stabb EV, Dunn AK. 2011. The haem-uptake gene cluster in *Vibrio fischeri* is regulated by Fur and contributes to symbiotic colonization. *Environ. Microbiol.* 13:2855–2864.

17. Wagner-Dobler I, Biebl H. 2006. Environmental biology of the marine *Roseobacter* lineage. *Annu. Rev. Microbiol.* 60:255–280.
18. Brinkhoff T, Giebel HA, Simon M. 2008. Diversity, ecology, and genomics of the *Roseobacter* clade: a short overview. *Arch. Microbiol.* 189:531–539.
19. Buchler J. 1975. Static coordination chemistry of metalloporphyrins, p 157–231. In Smith KM (ed), *Porphyrins and metalloporphyrins: a new edition based on the original volume*. Elsevier, New York, NY.
20. Price N, Harrison G, Hering J, Hudson R, Nirel P, Palenik B, Morel F. 1989. Preparation and chemistry of the artificial algal culture medium Aquil. *Biol. Oceanogr.* 6:443–461.
21. Hudson RJM, Morel FMM. 1989. Distinguishing between extracellular and intracellular iron in marine phytoplankton. *Limnol. Oceanogr.* 34:1113–1120.
22. Eddy SR. 2011. Accelerated profile HMM searches. *Plos Comput. Biol.* 7(10):e1002195. doi:10.1371/journal.pcbi.1002195.
23. Punta M, Coghill PC, Eberhardt RY, Mistry J, Tate J, Boursnell C, Pang N, Forslund K, Ceric G, Clements J, Heger A, Holm L, Sonnhammer ELL, Eddy SR, Bateman A, Finn RD. 2012. The Pfam protein families database. *Nucleic Acids Res.* 40:D290–D301.
24. Altschul SF, Madden TL, Schaffer AA, Zhang JH, Zhang Z, Miller W, Lipman DJ. 1997. Gapped BLAST and PSI-BLAST: a new generation of protein database search programs. *Nucleic Acids Res.* 25:3389–3402.
25. Wu CH, Apweiler R, Bairoch A, Natale DA, Barker WC, Boeckmann B, Ferro S, Gasteiger E, Huang HZ, Lopez R, Magrane M, Martin MJ, Mazumder R, O'Donovan C, Redaschi N, Suzek B. 2006. The Universal Protein Resource (UniProt): an expanding universe of protein information. *Nucleic Acids Res.* 34:D187–D191.
26. Desroche N, Beltramo C, Guzzo J. 2005. Determination of an internal control to apply reverse transcription quantitative PCR to study stress response in the lactic acid bacterium *Oenococcus oeni*. *J. Microbiol. Methods* 60:325–333.
27. Chang Q, Amemiya T, Liu JB, Xu XJ, Rajendran N, Itoh K. 2009. Identification and validation of suitable reference genes for quantitative expression of xylA and xylE genes in *Pseudomonas putida* mt-2. *J. Biosci. Bioeng.* 107:210–214.
28. Caporaso JG, Bittinger K, Bushman FD, DeSantis TZ, Andersen GL, Knight R. 2010. PyNAST: a flexible tool for aligning sequences to a template alignment. *Bioinformatics* 26:266–267.
29. Stamatakis A. 2006. RAXML-VI-HPC: maximum likelihood-based phylogenetic analyses with thousands of taxa and mixed models. *Bioinformatics* 22:2688–2690.
30. Sun SL, Chen J, Li WZ, Altintas I, Lin A, Peltier S, Stocks K, Allen EE, Ellisman M, Grethe J, Wooley J. 2011. Community cyberinfrastructure for advanced microbial ecology research and analysis: the CAMERA resource. *Nucleic Acids Res.* 39:D546–D551.
31. Whelan S, Goldman N. 2001. A general empirical model of protein evolution derived from multiple protein families using a maximum-likelihood approach. *Mol. Biol. Evol.* 18:691–699.
32. Wyckoff EE, Schmitt M, Wilks A, Payne SM. 2004. HtzZ is required for efficient heme utilization in *Vibrio cholerae*. *J. Bacteriol.* 186:4142–4151.
33. Han MV, Zmasek CM. 2009. phyloXML: XML for evolutionary biology and comparative genomics. *BMC Bioinformatics* 10:356. doi:10.1186/1471-2105-10-356.
34. Tai V, Palenik B. 2009. Temporal variation of *Synechococcus* clades at a coastal Pacific Ocean monitoring site. *ISME J.* 3:903–915.
35. Larkin MA, Blackshields G, Brown NP, Chenna R, McGettigan PA, McWilliam H, Valentin F, Wallace IM, Wilm A, Lopez R, Thompson JD, Gibson TJ, Higgins DG. 2007. Clustal W and clustal X version 2.0. *Bioinformatics* 23:2947–2948.
36. Rusch DB, Halpern AL, Sutton G, Heidelberg KB, Williamson S, Yooseph S, Wu DY, Eisen JA, Hoffman JM, Remington K, Beeson K, Tran B, Smith H, Baden-Tillson H, Stewart C, Thorpe J, Freeman J, Andrews-Pfannkoch C, Venter JE, Li K, Kravitz S, Heidelberg JF, Utterback T, Rogers YH, Falcon LI, Souza V, Bonilla-Rosso G, Eguiarte LE, Karl DM, Sathyendranath S, Platt T, Bermingham E, Gallardo V, Tamayo-Castillo G, Ferrari MR, Strausberg RL, Neelson K, Friedman R, Frazier M, Venter JC. 2007. The Sorcerer II Global Ocean Sampling expedition: northwest Atlantic through eastern tropical Pacific. *Plos Biol.* 5(3):e77. doi:10.1371/journal.pbio.0050077.
37. Matsen FA, Kodner RB, Armbrust EV. 2010. pplacer: linear time maximum-likelihood and Bayesian phylogenetic placement of sequences onto a fixed reference tree. *BMC Bioinformatics* 11:538. doi:10.1186/1471-2105-11-538.
38. Biers EJ, Sun SL, Howard EC. 2009. Prokaryotic genomes and diversity in surface ocean waters: interrogating the Global Ocean Sampling metagenome. *Appl. Environ. Microbiol.* 75:2221–2229.
39. Hopkins BM, Barbeau KA. 2012. Iron transporters in marine prokaryotic genomes and metagenomes. *Environ. Microbiol.* 14:114–128.
40. Stork M, Otto BR, Crosa JH. 2007. A novel protein, TtpC, is a required component of the TonB2 complex for specific iron transport in the pathogen *Vibrio anguillarum* and *Vibrio cholerae*. *J. Bacteriol.* 189:1803–1815.
41. Wiggerich HG, Klauke B, Koplán R, Priefer UB, Puhler A. 1997. Unusual structure of the tonB-*exb* DNA region of *Xanthomonas campestris* pv. *campestris*: tonB, *exbB*, and *exbD1* are essential for ferric iron uptake, but *exbD2* is not. *J. Bacteriol.* 179:7103–7110.
42. Wiggerich HG, Puhler A. 2000. The *exbD2* gene as well as the iron-uptake genes tonB, *exbB* and *exbD1* of *Xanthomonas campestris* pv. *campestris* are essential for the induction of a hypersensitive response on pepper (*Capsicum annuum*). *Microbiology* 146:1053–1060.
43. Alvarez B, Alvarez J, Menendez A, Guijarro JA. 2008. A mutant in one of two *exbD* loci of a TonB system in *Flavobacterium psychrophilum* shows attenuated virulence and confers protection against cold water disease. *Microbiology* 154:1144–1151.
44. Jasti S, Sieracki ME, Poulton NJ, Giewat MW, Rooney-Varga JN. 2005. Phylogenetic diversity and specificity of bacteria closely associated with *Alexandrium* spp. and other phytoplankton. *Appl. Environ. Microbiol.* 71:3483–3494.
45. Mayali X, Franks PJS, Azarn F. 2008. Cultivation and ecosystem role of a marine *Roseobacter* clade-affiliated cluster bacterium. *Appl. Environ. Microbiol.* 74:2595–2603.
46. Gonzalez JM, Simo R, Massana R, Covert JS, Casamayor EO, Pedros-Alio C, Moran MA. 2000. Bacterial community structure associated with a dimethylsulfoniopropionate-producing North Atlantic algal bloom. *Appl. Environ. Microbiol.* 66:4237–4246.
47. Toulza E, Tagliabue A, Blain S, Piganeau G. 2012. Analysis of the global ocean sampling (GOS) project for trends in iron uptake by surface ocean microbes. *PLoS One* 7(2):30931. doi:10.1371/journal.pone.0030931.
48. Schauer K, Rodionov DA, de Reuse H. 2008. New substrates for TonB-dependent transport: do we only see the ‘tip of the iceberg’? *Trends Biochem. Sci.* 33:330–338.
49. Hasegawa Y, Martin JL, Giewat MW, Rooney-Varga JN. 2007. Microbial community diversity in the phycosphere of natural populations of the toxic alga, *Alexandrium fundyense*. *Environ. Microbiol.* 9:3108–3121.
50. Kirchman DL. 1996. Oceanography: microbial ferrous wheel. *Nature* 383:303–304.
51. Boyd PW, Ellwood MJ. 2010. The biogeochemical cycle of iron in the ocean. *Nat. Geosci.* 3:675–682.
52. Strzepek RF, Maldonado MT, Higgins JL, Hall J, Safi K, Wilhelm SW, Boyd PW. 2005. Spinning the “ferrous wheel”: the importance of the microbial community in an iron budget during the FeCycle experiment. *Global Biogeochem. Cycles* 19:GB4S26. doi:10.1029/2005GB002490.
53. Haygood MG, Holt PD, Butler A. 1993. Aerobactin production by a planktonic marine *Vibrio* sp. *Limnol. Oceanogr.* 38:1091–1097.
54. Azam F. 1998. Microbial control of oceanic carbon flux: the plot thickens. *Science* 280:694–696.
55. Azam F, Long RA. 2001. Oceanography: sea snow microcosms. *Nature* 414:495–498.